Work Order No. 582-15-54388-011
Contract # 582-15-50417
Project 2015-45
Task 4

Final Report
Improved OSAT, APCA and PSAT Algorithms for CAMx

PREPARED UNDER A CONTRACT FROM THE
TEXAS COMMISSION ON ENVIRONMENTAL QUALITY

The preparation of this report was financed through a contract from the State of Texas through the Texas Commission on Environmental Quality. The content, findings, opinions and conclusions are the work of the author(s) and do not necessarily represent findings, opinions or conclusions of the TCEQ.

Prepared for:
Jim Price
Texas Commission on Environmental Quality
121 Park 35 Circle MC 164
Austin, TX 78753

Prepared by:
Greg Yarwood and Bonyoung Koo
Ramboll Environ
773 San Marin Drive, Suite 2115
Novato, California, 94998

August 2015

06-35854K

RAMBOLL ENVIRON

CONTENTS

EXECUTIVE SUMMARY 1

1.0 INTRODUCTION 2

1.1 Ozone Formation and Source Apportionment in CAMx 2

1.2 Project Objectives 2

1.3 Report Organization 2

2.0 IMPROVEMENTS TO OSAT, APCA AND PSAT 3

2.1 Timeline of OSAT Development 3

2.2 OSAT 3

2.2.1 OSAT Overview 3

2.2.2 OSAT2 4

2.2.3 OSAT3 7

2.3 APCA 9

2.4 PSAT 9

3.0 EVALUATION OF THE UPDATED OZONE SOURCE APPORTIONMENT 11

3.1 Modeling Database 11

3.2 OSAT Configuration 13

3.3 Comparison of Ozone Apportionments with OSAT2 and OSAT3 15

4.0 CONCLUSION AND RECOMMENDATIONS 23

4.1 Recommendations 23

5.0 REFERENCES 24

TABLES

Table 2-1. Development timeline for OSAT methods showing when methods were released in which model version. 3

Table 3-1. WRF and CAMx model layer structure for the June 2012 episode. 12

Table 3-2. Comparison of OSAT3 and OSAT2 contributions to monthly average MDA8 O_3 for June, 2012, at all receptor locations. 16

FIGURES

Figure 2-1. The OSAT1 tracer scheme for ozone apportionment $PH_2O_2/PHNO_3$ is 4

Figure 2-2. Daytime reactions of ozone with HOx (OH and HO_2) showing potential for reformation of ozone or ozone destruction via peroxide formation. 6

Figure 2-3. The OSAT2 scheme for ozone apportionment 6

Figure 2-4. Correspondence between NOy species in CB6r2 and tracer families in OSAT3 with conversions between species/tracers shown by arrows. 8

Figure 2-5. The OSAT3 scheme for ozone source apportionment. RGN apportions the nitrogen in NO_2 whereas OON and OOV apportion the odd-oxygen in NO_2. 9

Figure 3-1. TCEQ 36/12/4 km CAMx nested modeling grids for the Texas ozone modeling of June 2012. 13

Figure 3-2. Source region map for the CAMx ozone source apportionment modeling. 14

Figure 3-3. Locations of receptors in the CAMx ozone source apportionment modeling. 14

Figure 3-4. Contributions to daily MDA8 O_3 in June, 2012 from sources outside the US, outside Texas and within Texas at three monitors downwind of urban areas: Eagle Mountain Lake (CAMS 75; top), Conroe (CAMS 78; middle) and San Antonio Northwest (CAMS 23; bottom). 17

Figure 3-5. Contributions to daily MDA8 O_3 in June, 2012 from sources outside the US, outside Texas and within Texas at three monitors in rural areas: Big Bend (CAMS 67; top), Palestine (CAMS 647; middle) and Aransas Pass (CAMS 659; bottom). 18

Figure 3-6. Hourly O_3 and OSAT3 tracers for Houston area emissions at 06:00 CST on June 14, 2012. Where the plume of O_3 from Houston emissions passes over the DFW metro area, a local minimum occurs where Houston O_3 has reacted with DFW NO emissions causing a local maximum in the tracer for odd-oxygen in NO_2 from Houston O_3. The tracer for Houston NO_2 has a different footprint because it traces the origin of nitrogen rather than the odd-oxygen in NO_2. 20

Figure 3-7. Hourly O_3 and OSAT3 tracers for Houston area emissions at 06:00 and 07:00 CST on June 14, 2012. Over the DFW metro area, decreases in the tracer for odd-oxygen in NO_2 from Houston O_3 coincide with increases in Houston O_3, as seen from the difference between OSAT3 and OSAT2, because OSAT3 attributes O_3 formed from destruction of NO_2 to the sources of odd-oxygen in the NO_2 destroyed. 21

Figure 3-8. Hourly O_3 and PAN attributed to Houston area emissions at 11:00 and 13:00 CST on June 16, 2012. In Oklahoma, decreased PAN corresponds to increased O_3 with OSAT3, as seen from the O_3 difference between OSAT3 and OSAT2, because OSAT3 accounts for NOx recycled from PAN and subsequent O_3 production from the NOx. 22

LIST OF ACRONYMS AND ABBREVIATIONS

AACOG	Alamo Area Council of Governments
APCA	Anthropogenic Precursor Culpability Assessment
BCs	Boundary Conditions
BPA	Beaumont-Port Arthur Area
CAMS	Continuous Air Monitoring Station
CAMx	Comprehensive Air quality Model with extensions
CAPCOG	Capital Area Council of Governments
CTCOG	Central Texas Council of Governments
DFW	Dallas-Fort Worth Area
EPA	Environmental Protection Agency
GEOS-Chem	Goddard Earth Orbiting System model with Chemistry
HGB	Houston-Galveston-Brazoria Area
HO_2	Hydroperoxy radical
HONO	Nitrous Acid
HNO_3	Nitric Acid
HOTCOG	Heart of Texas Council of Governments
ICs	Initial Conditions
KTF	Killeen-Temple-Fort Hood
LCC	Lambert Conic Conformal
MDA8	daily maximum 8-hour average
MEGAN	Model of Gases and Aerosols from Nature
NAA	Non-Attainment Area (for the ozone NAAQS)
NAAQS	National Ambient Air Quality Standard
NNA	Near Non-Attainment Area (for the ozone NAAQS)
NO	Nitric Oxide
NO_2	Nitrogen Dioxide
NO_3	Nitrogen Trioxide
N_2O_5	Dinitrogen Pentoxide
NOx	Oxides of Nitrogen (principally NO and NO_2)
NOy	Oxidized Nitrogen (principally NO, NO_2, NO_3, N_2O_5, HONO, HNO_3, PANs and ONs)
NOz	NOy minus NOx
$O(^1D)$	Oxygen atoms in an excited electronic state
$O(^3P)$	Oxygen atoms in the ground electronic state
O_3	Ozone
OH	Hydroxyl radical
ONs	Organic Nitrates
OSAT	Ozone Source Apportionment Technology
PANs	Peroxyacyl Nitrates (principally peroxyacetyl nitrate)
ppb	parts per billion
PSAT	PM Source Apportionment Technology
RPO	Regional Planning Organization

SIP	State Implementation Plan
TCEQ	Texas Commission on Environmental Quality
VOC	volatile organic compound
WRF	Weather Research and Forecast model

EXECUTIVE SUMMARY

The Texas Commission on Environmental Quality (TCEQ) uses the Comprehensive Air quality Model with extensions (CAMx) to support regulatory air quality requirements including developing State Implementation Plan (SIP) submittals. The TCEQ uses the CAMx Ozone Source Apportionment Technology (OSAT), Anthropogenic Precursor Culpability Assessment (APCA), and Particulate Matter Source Apportionment Technology (PSAT) to calculate quantitatively the source types and source areas contributing to ozone and particulate matter (PM) impacts at receptor locations.

Ozone (O_3) is formed in the atmosphere by reactions of nitrogen oxides (NOx) and volatile organic compounds (VOC) in the presence of sunlight. Once formed, O_3 persists and can be transported by prevailing winds. The OSAT, APCA, and PSAT algorithms in CAMx (collectively the OSAT methods) use tracers to keep track of O_3 production and transport.

In this project the OSAT methods were successfully updated to include source apportionment of nitrogen dioxide (NO_2). The sources of both the nitrogen atom and the odd oxygen atom in NO_2 are attributed, and these source profiles will almost always differ. The modifications improve the accuracy of the ozone source apportionment in two ways:

- By keeping track of the source(s) of O_3 removed by reaction with NO to form NO_2 and subsequently returned as O_3 when the NO_2 is destroyed by photolysis.
- By keeping track of so-called "NOx recycling," when NOx is converted to a different form of oxidized nitrogen, such as NHO_3, and later converted back to NOx.

The effect of these updates on O_3 source attribution is that the contribution of local emissions generally is reduced and the contribution of transported O_3 generally is increased.

1.0 INTRODUCTION

The Texas Commission on Environmental Quality (TCEQ) uses the Comprehensive Air quality Model with extensions (CAMx) to support regulatory air quality requirements including developing State Implementation Plan (SIP) submittals. The TCEQ uses the CAMx Ozone Source Apportionment Technology (OSAT), Anthropogenic Precursor Culpability Assessment (APCA), and Particulate Matter Source Apportionment Technology (PSAT) to calculate quantitatively the source types and source areas contributing to ozone and particulate matter (PM) impacts at receptor locations.

1.1 Ozone Formation and Source Apportionment in CAMx

Ozone (O_3) is formed in the atmosphere by reactions of nitrogen oxides (NOx) and volatile organic compounds (VOC) in the presence of sunlight. Once formed, O_3 persists and can be transported by prevailing winds. The OSAT, APCA, and PSAT algorithms in CAMx (collectively the OSAT methods) use tracers to keep track of O_3 production and transport (Yarwood et al., 1996; ENVIRON, 2015).

The OSAT methods perform source attribution of O_3 within a CAMx simulation, i.e., they provide a quantitative accounting of where O_3 originated for any and all locations in the CAMx simulation. Within photochemical models like CAMx, O_3 can originate from the initial conditions, the boundary conditions and emissions of ozone precursors (NOx and VOC). The OSAT methods allow the emission inventory to be disaggregated to geographic regions and/or source categories for purposes of source apportionment.

1.2 Project Objectives

When O_3 is transported into NOx-rich areas it can be converted to nitrogen dioxide (NO_2) by reaction with locally emitted nitric oxide (NO). In this circumstance, OSAT, APCA, and PSAT treat the transported O_3 as having been destroyed and any O_3 formed subsequently by photolyzing the NO_2 is considered to be new O_3 and likely attributed to local emission sources. The primary objective of this study was to improve the accuracy of the OSAT methods by keeping track of the source(s) of O_3 removed by reaction with NO to form NO_2 and subsequently returned as O_3 when the NO_2 is destroyed by photolysis.

Adding NO_2 apportionment to the OSAT methods required instituting more complete tracking of how emissions of NOx (NO and NO_2) are converted to and from other chemical forms of oxidized nitrogen. This update produced an additional improvement in the accuracy of the OSAT methods by keeping track of so-called “NOx recycling,” when NOx is converted to a different form of oxidized nitrogen, such as NHO_3, and later converted back to NOx.

1.3 Report Organization

This section provides background information and describes the purpose of this project. Section 2 describes the OSAT, APCA and PSAT methods and explains what updates were made in this project. Section 3 shows the results of testing the new OSAT method in CAMx. Section 4 presents our conclusions and recommendations for future work.

2.0 IMPROVEMENTS TO OSAT, APCA AND PSAT

ENVIRON developed an O_3 source attribution approach that has become known as the "Ozone Source Apportionment Technology", or OSAT (Yarwood et al., 1996). This method was originally implemented in the Urban Airshed Model (UAM) and was built into the first version of CAMx. OSAT provides a method for estimating the contributions of multiple source areas, categories, and pollutant types to O_3 formation in a single model run.

2.1 Timeline of OSAT Development

The development timeline for the OSAT methods is summarized in Table 2-1.The original development of OSAT occurred in 1995 with UAM and the first release of CAMx in 1996 included OSAT. APCA was released in 1997 as a variant of OSAT to provide source attributions that are more policy relevant because certain source categories, namely biogenic emissions, are considered non-controllable.

The second version of OSAT (OSAT2) was released in 2005 along with PSAT. The OSAT2 update accounted for simultaneous production and destruction of O_3 by photochemistry and, compared to the first version of OSAT, tended to allocate less O_3 to long-range transport (because of O_3 destruction during transport) and more to local production. The term "OSAT2" was not used widely but the update was announced and described in the User's Guide for CAMx 4.2. The OSAT2 update was also incorporated into APCA and PSAT and these are the versions of the OSAT methods in CAMx 6.2 which was the starting point for this project.

The third version of OSAT developed in this project is called OSAT3. The OSAT3 update is incorporated into APCA and PSAT.

Table 2-1. Development timeline for OSAT methods showing when methods were released in which model version.

1995	1996	1997	2005	2015
OSAT	OSAT	APCA	"OSAT2" & PSAT	"OSAT3"
UAM-IV	CAMx 1.1	CAMx 2.0	CAMx 4.2	CAMx 6.3 (planned)

2.2 OSAT

2.2.1 OSAT Overview

OSAT uses multiple tracer species to track the fate of O_3 precursor emissions (VOC and NOx) and the O_3 formation caused by these emissions within a simulation. The tracers operate as spectators to the normal CAMx calculations so that the underlying CAMx predicted relationships between emission groups (sources) and O_3 concentrations at specific locations (receptors) are not perturbed. The tracers allow O_3 formation from multiple "source groups" to be tracked simultaneously within a single simulation. A source group can be defined in terms of geographical area and/or emission category.

OSAT uses four tracers per source group to account for contributions to O_3 formation. O_3 formation involves both NOx and VOC, and the NOx and VOC participating in O_3 formation in any particular grid cell/time step may have originated from different source groups. OSAT uses two tracer families (N_i and V_i) to apportion NOx and VOC by source group *i*. The O_3 formation process can be controlled more by the availability of VOCs or NOx, depending upon the relative abundance of both precursors, and O_3 formation is described either as VOC-limited or NOx-limited, respectively. When O_3 production at a given location and time is NOx-limited, it makes sense to attribute O_3 production to source groups based on their contributions to the local NOx, and similarly to allocate based on VOC contributions when O_3 formation is VOC-limited. Consequently, separate O_3 tracer families ($O3N_i$ and $O3V_i$) are used to track O_3 formed under NOx and VOC-limited conditions.

The OSAT1 tracer families for ozone apportionment are:

N_i	Nitric oxide (NO) and nitrogen dioxide (NO_2) emitted by source group *i*
V_i	VOC emitted by source group *i*
$O3N_i$	O_3 formed under NOx-limited conditions from N_i
$O3V_i$	O_3 formed under VOC-limited conditions from V_i

The indicator used to classify O_3 formation as being instantaneously limited by NOx or VOC is the ratio of the production rates of hydrogen peroxide (H_2O_2) and HNO_3 ($PH_2O_2/PHNO_3$). O_3 formation is classified as being NOx-limited when the ratio $PH_2O_2/PHNO_3$ is less than 0.35 (Sillman, 1995).

The OSAT1 tracer scheme for ozone apportionment is illustrated in Figure 2-1. O_3 changes due to chemistry (ΔO_3) are tracked by the tracer families O3N and O3V. Ozone destruction (i.e., $\Delta O_3 < 0$) reduces all O3N and O3V proportionately. O_3 production (i.e., $\Delta O_3 > 0$) is classified either as NOx-limited or VOC-limited using the indicator $PH_2O_2/PHNO_3$ and assigned either to O3N or O3V, respectively, in proportion to the precursor tracers present, respectively N or V. The precursor tracers V and N are removed by chemical decay.

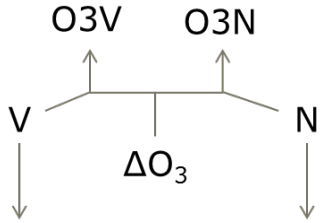

Figure 2-1. The OSAT1 tracer scheme for ozone apportionment $PH_2O_2/PHNO_3$ is

2.2.2 OSAT2

The original OSAT algorithm allocated the net change in O_3 (ΔO_3) to tracers O3N and/or O3V. However, ozone production and destruction reactions operate simultaneously and so the net

change in O_3 is the balance of production and destruction. For example, VOC oxidation can cause photochemical O_3 production at the same time that O_3 + VOC reactions directly consume O_3, and these processes may lead to a net increase or decrease in O_3 depending mainly upon availability of NOx and sunlight.

OSAT2 accounts for the following ozone destruction mechanisms:

1) O_3 + VOC reactions since these remove ozone;
2) $O(^3P)$ + VOC reactions since these effectively remove ozone;
3) $O(^1D)$ + H_2O reaction since this effectively removes ozone;
4) HOx + O_3 reactions that do not re-form ozone.

O_3 destruction is calculated as the smaller (i.e., more negative) of the sum of these four mechanisms or ΔO_3. O_3 production is then calculated as the difference between ΔO_3 and the ozone destruction. The O3V and O3N tracers are adjusted first for O_3 destruction (applied to all tracers) and second for O_3 production (applied using the OSAT or APCA rules).

The amount of O_3 destruction is calculated from the time-integrated rates of the four chemical processes listed above. It is easy to account for processes 1-3 since the ozone destroyed is simply the time-integral of the reactions involved. Process 4 is less easy to quantify because O_3 can be re-formed. For example:

$O_3 + OH \rightarrow HO_2$

$HO_2 + NO \rightarrow OH + NO_2$

$NO_2 + h\nu \rightarrow NO + O$

$O + O_2 \rightarrow O_3$

However, process 4 is an important O_3 destruction mechanism in low NOx (e.g., rural) environments. Therefore, accounting for process 4 is important to understanding long-range O_3 transport. The main reaction pathways between O_3 and HOx (OH and HO_2) are shown in Figure 2-2. The ozone destruction rate due to O_3 + HOx reactions is computed as:

$$\mathrm{O_3\ Destruction} = \mathrm{Rate}_{(O_3 + HOx)} \times \left(\frac{\mathrm{Rate}_{(HO_2\ term)}}{\mathrm{Rate}_{(HO_2 + NO)} + \mathrm{Rate}_{(HO_2\ term)}} \right)$$

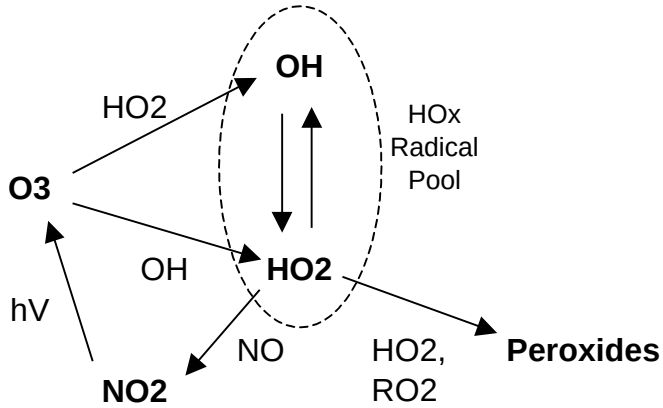

Figure 2-2. Daytime reactions of ozone with HOx (OH and HO_2) showing potential for reformation of ozone or ozone destruction via peroxide formation.

The OSAT2 tracer families for O_3 apportionment are the same as for OSAT1, namely:

N_i	Nitric oxide (NO) and nitrogen dioxide (NO_2) emitted by source group *i*
V_i	VOC emitted by source group *i*
$O3N_i$	Ozone formed under NOx-limited conditions from N_i
$O3V_i$	Ozone formed under VOC-limited conditions from V_i

The OSAT2 scheme for O_3 apportionment is illustrated in Figure 2-3. O_3 production and destruction are treated separately and can occur simultaneously. Ozone destruction ($-\Delta O_3$) reduces all O3N and O3V proportionately. O_3 production ($+\Delta O_3$) is classified either as NOx-limited or VOC-limited using the indicator $PH_2O_2/PHNO_3$ and assigned either to O3N or O3V, respectively, in proportion to the precursor tracers present, respectively N or V. The precursor tracers V and N are removed by chemical decay.

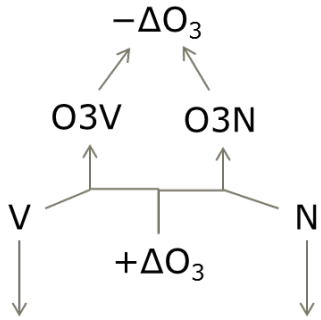

Figure 2-3. The OSAT2 scheme for ozone apportionment

2.2.3 OSAT3

The objective of this project is to improve the accuracy of the OSAT methods by keeping track of the source(s) of O_3 removed by reaction with NO to form NO_2 and subsequently returned as O_3 when the NO_2 is destroyed by photolysis. Accomplishing this objective requires maintaining source attribution of odd-oxygen through the chemical reactions that link O_3, NO and NO_2. This is illustrated in the following chemical reactions where O_3 is written as OOO, NO_2 is written as ONO, and the source attributed odd-oxygen is shown in red:

NO + OOO → ONO

ONO + hv → NO + O

O + OO → OOO

Source attribution of the odd-oxygen content of NO_2 is performed by tracer families OON and OOV that are newly introduced in OSAT3. Two tracer families are needed in order to keep track of the source profile of O_3 consumed which was represented by O3V and O3N .

Source attribution of the nitrogen in NO and NO_2 must also be performed in order to apply the OSAT or APCA algorithms that track O_3 production using O3N and O3V. Accordingly, OSAT3 simultaneously attributes both the N and odd-oxygen in NO_2 to sources, and the source signatures of these two apportionments will almost always differ. This is illustrated in the following chemical source attribution is shown by blue for nitrogen and by red for odd-oxygen:

NO + OOO → ONO

ONO + hv → NO + O

O + OO → OOO

The chemical conversion pathways between oxidized nitrogen species (NOy) in CB6r2 are summarized in Figure 2-4. Arrows show the direction of conversion which is bi-directional in some cases. Other chemical mechanisms have similar NOy conversion pathways to CB6r2. Also shown in Figure 2-4 are the OSAT3 tracer families. Color coding shows the correspondence between OSAT3 tracer families and the NOy species that they represent (but this color coding is different from the chemical reactions above because it has a different purpose).

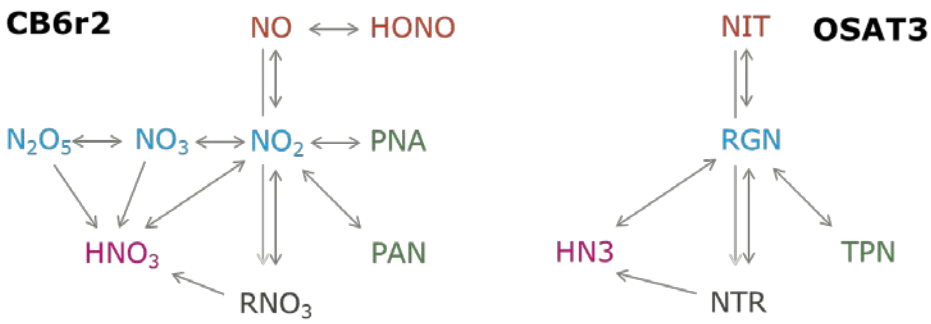

Figure 2-4. Correspondence between NOy species in CB6r2 and tracer families in OSAT3 with conversions between species/tracers shown by arrows.

Tracking source attribution of nitrogen through all forms of NOy enables OSAT3 to account for NOx recycling when NOx is converted to another form of NOy (e.g., PAN or HNO_3) and later converted back to NOx. OSAT3 uses the following 10 tracer families for O_3 source apportionment:

V_i	VOC emitted by source group *i*
NIT_i	Nitric oxide (NO) and nitrous acid (HONO)
RGN_i	Nitrogen dioxide, nitrate radical (NO_3) and dinitrogen pentoxide (N_2O_5)
TPNi	Peroxyl acetyl nitrate (PAN), analogues of PAN and peroxy nitric acid (PNA)
NTRi	Organic nitrates (RNO_3)
HN3i	Gaseous nitric acid (HNO_3)
$O3N_i$	O_3 formed under NOx-limited conditions from N_i
$O3V_i$	O_3 formed under VOC-limited conditions from V_i
OON_i	Odd-oxygen in NO_2 formed from $O3N_i$
OOV_i	Odd-oxygen in NO_2 formed from $O3V_i$

The nitrogen tracer families for OSAT3 are very similar to the existing PSAT tracer families for particulate nitrate (discussed below) with the only difference being the addition of tracer family NIT in OSAT3. Therefore, PSAT has been updated to use the OSAT3 tracer families for oxidized nitrogen.

The OSAT3 scheme for O_3 apportionment is illustrated in Figure 2-5. The VOC precursor tracer family V is removed by chemical decay. The fate of NOx emissions is tracked by the nitrogen tracer families NIT, RGN, TPN, NTR and HN3. O_3 production and destruction are treated separately and can occur simultaneously. O_3 production ($+\Delta O_3$) is classified either as NOx-limited or VOC-limited using the indicator $PH_2O_2/PHNO_3$ and assigned either to O3N or O3V, respectively, in proportion to the precursor tracers present, respectively NIT or V. O_3 destruction ($-\Delta O_3$) reduces all O3N and O3V proportionately. When O_3 destruction results from reaction with NO to form NO_2, the amounts of O3N and O3V removed are transferred to the respective odd-oxygen tracers OON and OOV. When NO_2 is removed by photolysis to form O_3,

the amounts of OON and OOV removed are transferred to the respective O_3 tracers OON and OOV.

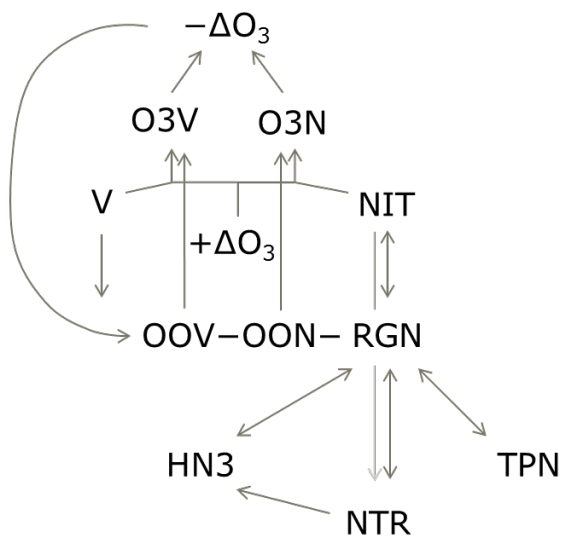

Figure 2-5. The OSAT3 scheme for ozone source apportionment. RGN apportions the nitrogen in NO_2 whereas OON and OOV apportion the odd-oxygen in NO_2.

2.3 APCA

APCA differs from OSAT in recognizing that certain emission categories are not controllable (e.g., biogenic emissions) and that apportioning O_3 production to these categories does not provide information that is relevant to development of control strategies. To address this, in situations where OSAT would attribute O_3 production to non-controllable emissions, APCA re-allocates that O_3 production to the controllable precursors that participated in O_3 formation with the non-controllable precursor. For example, when O_3 formation is due to biogenic VOC and anthropogenic NOx under VOC-limited conditions (a situation in which OSAT would attribute O_3 production to biogenic VOC), APCA attributes O_3 production to the NOx precursors present. Using APCA instead of OSAT results in more O_3 formation attributed to anthropogenic NOx sources and less O_3 formation attributed to biogenic VOC sources.

The only difference between APCA and OSAT is the algorithm used to allocate ozone production under VOC or NOx-limited conditions. The OSAT3 update does not revise the allocation of ozone production under VOC or NOx-limited conditions and therefore the APCA algorithm works with the OSAT3 update.

2.4 PSAT

PSAT uses multiple tracers to track the fate of primary and secondary PM. PSAT can apportion the following categories of PM:

- Primary PM
- Sulfate (PSO4)
- Particulate nitrate (PNO3)
- Ammonium (PNH4)
- Secondary organic aerosol (SOA)
- Particulate mercury (HgP)

A single tracer family can apportion primary PM species whereas secondary PM species require several tracer families to track the relationship between gaseous precursors and the resulting PM. PNO3 and SOA are the most complex PM categories to apportion because the emitted precursor gases (NO, VOC) are several steps removed from the resulting PM species (PNO3, SOA).

Both O_3 and PNO3 are associated with NOx emissions. The PSAT tracers for the PNO3 category are listed below. PSAT tracer names for particulate species generally begin with the letter "P."

RGN_i	Reactive gaseous nitrogen, namely nitric oxide (NO), nitrogen dioxide (NO_2), nitrate radical (NO_3), dinitrogen pentoxide (N_2O_5) and nitrous acid (HONO)
TPNi	Peroxyl acetyl nitrate (PAN), analogues of PAN and peroxy nitric acid (PNA)
NTRi	Organic nitrates (RNO_3)
HN3i	Gaseous nitric acid (HNO_3)
PN3i	Particulate nitrate ion from primary emissions plus secondarily formed nitrate
NH3i	Gaseous ammonia (NH_3)
PN4i	Particulate ammonium ion (NH_4)

The oxidized nitrogen tracer families for OSAT3 and PSAT are very similar with the only difference being the additional tracer family NIT in OSAT3. Therefore, PSAT has been updated to use the OSAT3 tracer families for oxidized nitrogen.

3.0 EVALUATION OF THE UPDATED OZONE SOURCE APPORTIONMENT

We tested the updated OSAT3 source apportionment method using version 6.2 of CAMx with a modeling database for June, 2012, developed by the TCEQ. [1]

3.1 Modeling Database

The TCEQ nested grid modeling domain for the June 2012 episode is shown in Figure 3-1. The outer 36 km domain shown in black in Figure 3-1 encompasses the continental US (CONUS) so that the model boundary conditions represent essentially the non-North American contribution to O_3. The 12 km grid (shown in blue in Figure 3-1) includes all of Texas plus a substantial area that would be upwind of Texas during an ozone episode. This is important to accurately represent any influence of ozone transport since ozone formation is modeled more accurately by a 12 km grid than a 36 km grid. The intention is to accurately model potential transport of ozone from areas at a distance upwind from Texas of about the breadth of one state. The 4 km grid shown in blue in Figure 3-2 was not used in this study.

The TCEQ developed meteorological input data for CAMx using the Weather Research and Forecast (WRF) meteorological model version 3.6.1 (Skamarock et al., 2005) and then processed WRF outputs using the WRFCAMx preprocessor. Table 3-1 shows the vertical layer systems for the WRF and CAMx modeling. The TCEQ developed boundary conditions for the 36 km grid using the Goddard Earth Orbiting System model with Chemistry (GEOS-Chem; Bey et al., 2001) global chemistry-transport model. The TCEQ developed the biogenic emission inputs for CAMx using the Model of Gases and Aerosols from Nature (MEGAN; Guenther et al., 2012) and the anthropogenic emission inputs using data from the TCEQ and EPA.

[1] ftp://amdaftp.tceq.texas.gov/pub/TX/camx/basecase/bc12_12jun.reg3a.2012_wrf361_p2a_i2_a/

Table 3-1. WRF and CAMx model layer structure for the June 2012 episode.[2]

Vertical Layer Structure

Corresponding WRF Layer	Layer Top (m AGL)	CAMx Layer	Layer Center (m AGL)	Thickness (m)
38	15179.1	28	13637.9	3082.5
36	12096.6	27	10631.6	2930.0
32	9166.6	26	8063.8	2205.7
29	6960.9	25	6398.4	1125.0
27	5835.9	24	5367.0	937.9
25	4898.0	23	4502.2	791.6
23	4106.4	22	3739.9	733.0
21	3373.5	21	3199.9	347.2
20	3026.3	20	2858.3	335.9
19	2690.4	19	2528.3	324.3
18	2366.1	18	2234.7	262.8
17	2103.3	17	1975.2	256.2
16	1847.2	16	1722.2	249.9
15	1597.3	15	1475.3	243.9
14	1353.4	14	1281.6	143.6
13	1209.8	13	1139.0	141.6
12	1068.2	12	998.3	139.7
11	928.5	11	859.5	137.8
10	790.6	10	745.2	90.9
9	699.7	9	654.7	90.1
8	609.7	8	565.0	89.3
7	520.3	7	476.1	88.5
6	431.8	6	387.9	87.8
5	344.0	5	300.5	87.1
4	256.9	4	213.8	86.3
3	170.6	3	127.8	85.6
2	85.0	2	59.4	51.0
1	33.9	1	17.0	33.9

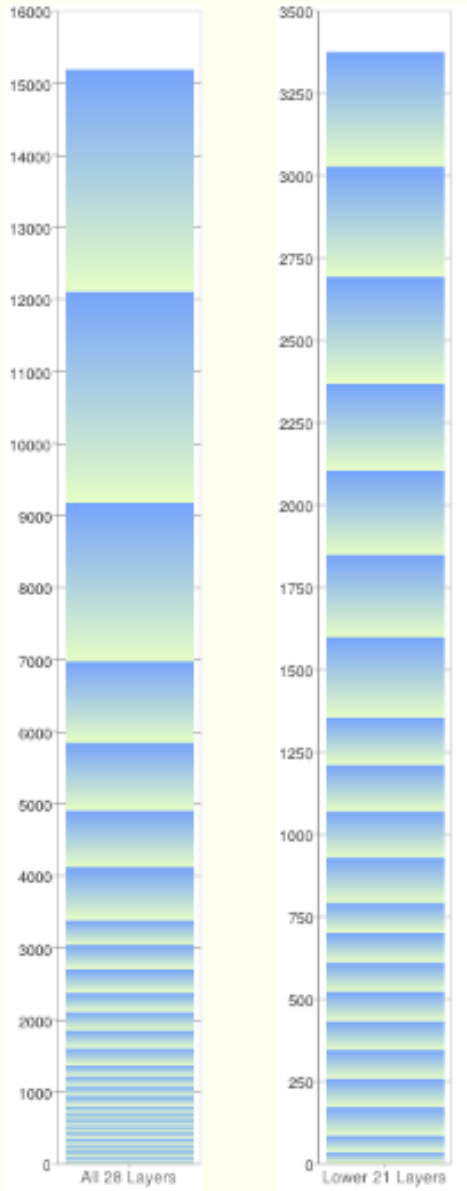

AGL - Above Ground Level.

[2] TCEQ figure from http://www.tceq.texas.gov/airquality/airmod/rider8/modeling/domain

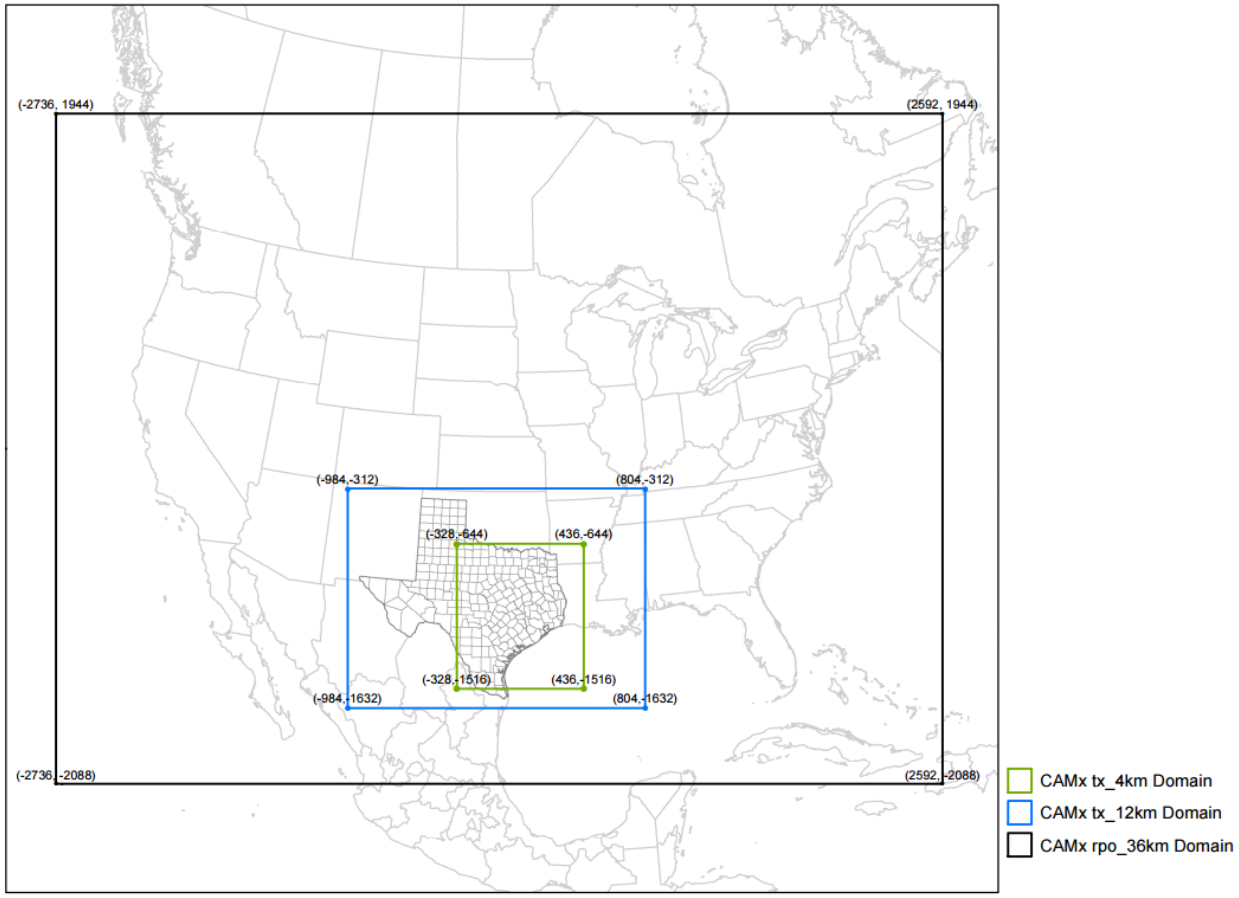

Figure 3-1. TCEQ 36/12/4 km CAMx nested modeling grids for the Texas ozone modeling of June 2012.[3]

3.2 OSAT Configuration

Figure 3-2 shows the source region map used in the CAMx ozone source apportionment analysis. The map shows the outline of the CAMx 12 km boundary in red and 4 km boundary in blue. All areas outside the 12 km grid that are not part of Mexico are defined to be part of the "Other" source region. Figure 3-3 shows locations of 23 receptors selected for the analysis of CAMx ozone source apportionment results.

[3] TCEQ figure from http://www.tceq.texas.gov/airquality/airmod/rider8/modeling/domain

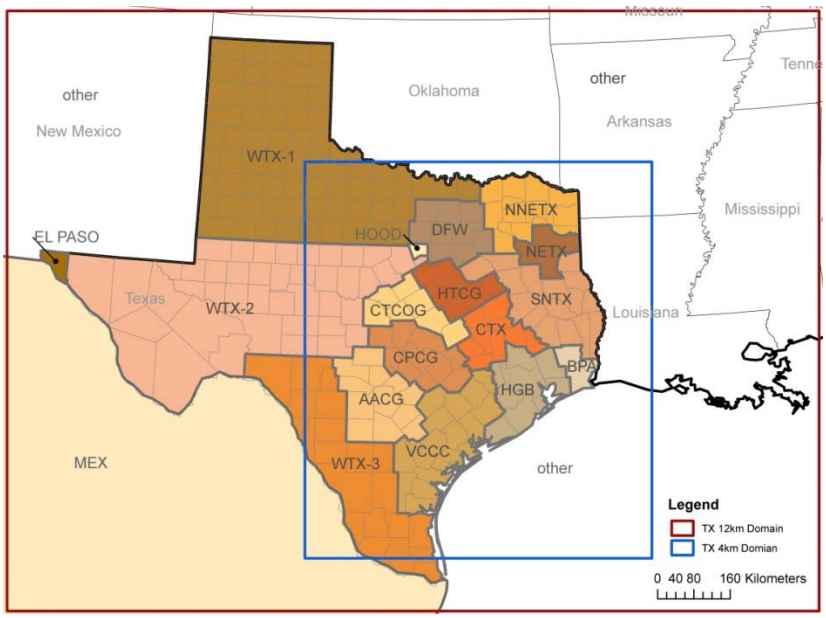

Figure 3-2. Source region map for the CAMx ozone source apportionment modeling.

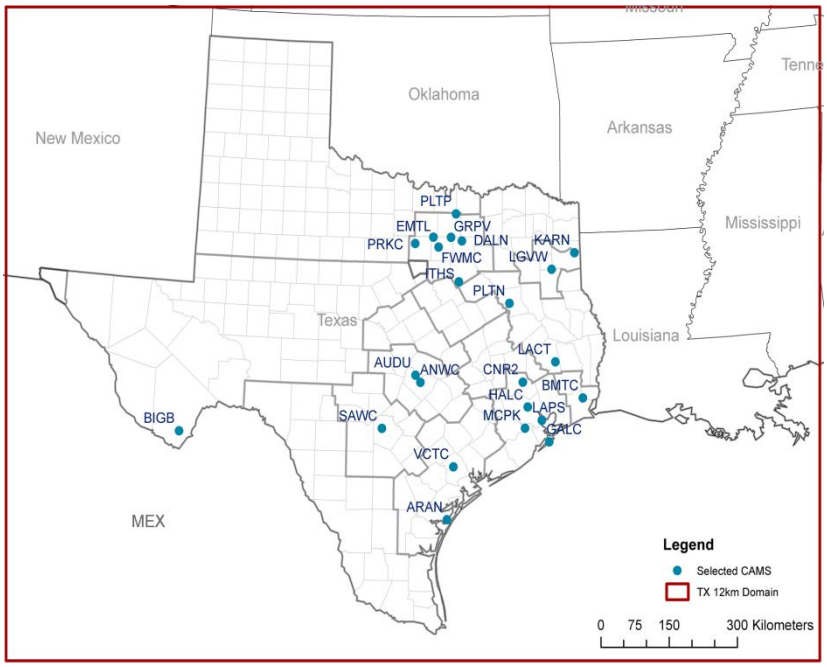

Figure 3-3. Locations of receptors in the CAMx ozone source apportionment modeling.

3.3 Comparison of Ozone Apportionments with OSAT2 and OSAT3

Our evaluation of CAMx model results is based on daily maximum 8-hour average (MDA8) O_3 because this quantity is used to assess compliance with the National Ambient Air Quality Standard (NAAQS) for O_3. The average modeled MDA8 O_3 for the 23 selected receptor locations (Figure 3-3) is shown in Table 3-2. Also shown in Table 3-2 are the following source contributions determined by OSAT2 and OSAT3:

- The local area contribution is the O_3 attributed to emissions within the source region containing the receptor
- The contribution of boundary conditions is the O_3 that entered the 36 km CAMx grid with prevailing winds plus any O_3 formed within the CAMx domain from precursors that entered the 36 km CAMx grid with prevailing winds
- The contribution from emissions outside Texas is the O_3 formed from emissions within the Mexico and "other" source regions shown in Figure 3-2.

At all receptors the local area contribution to monthly average MDA8 O_3 is smaller with OSAT3 than OSAT2. The largest reduction of 1.2 ppb occurs at Eagle Mountain Lake (CAMS 75) and Pilot Point (CAMS 1032) receptors which are both downwind of the DFW area on many high ozone days. The reduction is 1.1 ppb at the Conroe monitor (CAMS 78) downwind of Houston and 0.8 ppb at the San Antonio Northwest monitor (CAMS 23) downwind of San Antonio. Daily MDA8 O_3 contributions with OSAT2 and OSAT3 are compared in Figure 3-4 for three monitors that tend to be downwind of urban areas: Eagle Mountain Lake (CAMS 75), Conroe (CAMS 78) and San Antonio Northwest (CAMS 23) and Figure 3-5 compares three monitors that are outside urban areas:Big Bend (CAMS 67), Palestine (CAMS 647) and Aransas Pass (CAMS 659). On all days at all six monitors, the ozone contribution of emissions within Texas is smaller with OSAT3 than OSAT2.

The smaller local area contribution to monthly average MDA8 O_3 with OSAT3 than OSAT2 is exactly offset by larger contributions from outside the local area. Table 3-2 shows that the contribution of boundary conditions is always higher with OSAT3 by 0.7 to 1.2 ppb and the contribution of emissions from outside Texas is larger with OSAT3 at most receptor locations. Three receptors that exemplify smaller contributions from emissions outside Texas with OSAT3 than OSAT2 are Galveston (CAMS 34), Karnack (CAMS 85) and Beaumont Lamar (CAMS 2). These receptors are all located near the periphery of the Texas source regions (Figure 3-3) meaning that emissions from outside Texas are to some extent "local" to these receptors, and that the reduced contribution of emissions outside Texas corresponds to the reduced contribution of local emissions seen at all receptors.

Table 3-2. Comparison of OSAT3 and OSAT2 contributions to monthly average MDA8 O_3 for June, 2012, at all receptor locations.

Receptor, CAMS Number	Local Area	CAMx MDA8 O_3 (ppb)	Local Area Contribution to MDA8 O_3 (ppb)			Boundary Condition Contribution to MDA8 O_3 (ppb)			Contribution of Emissions Outside Texas to MDA8 O_3 (ppb)		
			OSAT2	OSAT3	Change	OSAT2	OSAT3	Change	OSAT2	OSAT3	Change
Italy High School, C650	DFW	55	3.2	2.9	-0.3	21.8	22.7	1.0	15.1	15.7	0.6
Parker County, C76	DFW	56	8.5	7.7	-0.8	20.0	20.9	0.9	13.0	13.8	0.8
Eagle Mountain Lake, C75	DFW	62	14.8	13.6	-1.2	20.4	21.4	1.0	14.5	15.2	0.7
Ft. Worth Northwest, C13	DFW	62	15.1	14.4	-0.8	20.3	21.2	0.9	14.7	15.2	0.5
Pilot Point, C1032	DFW	63	12.8	11.5	-1.2	20.3	21.4	1.1	16.8	17.5	0.7
Dallas North, C63	DFW	63	14.1	13.5	-0.7	20.9	21.8	0.9	16.6	17.0	0.4
Grapevine Fairway, C70	DFW	65	17.7	16.6	-1.1	20.8	21.9	1.1	15.8	16.4	0.6
Manvel Croix Park, C84	HGB	60	15.9	15.0	-0.8	17.3	18.3	1.0	23.0	22.9	-0.1
Conroe Relocated, C78	HGB	62	19.8	18.7	-1.1	17.0	18.2	1.2	20.7	21.0	0.3
Houston Aldine, C8	HGB	62	20.8	20.0	-0.8	17.2	18.2	1.0	20.8	20.8	0.0
La Porte Sylvan Beach, C556	HGB	63	15.1	14.6	-0.5	17.4	18.4	1.0	25.8	25.5	-0.3
Galveston Airport, C34	HGB	64	10.7	10.5	-0.2	17.9	18.9	1.0	31.1	30.3	-0.8
Longview, C19	NETX	60	7.7	7.1	-0.6	20.4	21.3	1.0	22.4	22.6	0.2
Karnack, C85	NETX	62	4.8	4.7	-0.1	18.7	19.8	1.1	30.1	29.6	-0.6
Palestine, C647	SNTX	53	4.5	3.7	-0.8	20.4	21.3	0.9	18.4	19.0	0.5
Alabama Coushatta, C1027	SNTX	53	4.3	3.8	-0.6	18.3	19.3	1.0	22.7	22.7	0.0
Beaumont Lamar, C2	BPA	58	9.7	9.5	-0.2	18.1	19.1	0.9	27.1	26.4	-0.6
Austin Northwest, C3	CTX	56	0.6	0.5	-0.1	20.6	21.4	0.8	13.9	14.3	0.4
Audubon, C38	CTX	57	0.6	0.6	-0.1	21.4	22.3	0.9	13.6	14.1	0.4
San Antonio Northwest, C23	AACG	57	15.8	14.9	-0.8	20.3	21.1	0.9	13.0	13.4	0.4
Aransas Pass, C659	VCCC	45	3.6	3.2	-0.3	19.2	19.8	0.7	19.5	19.3	-0.2
Victoria, C87	VCCC	48	6.9	6.3	-0.6	19.0	19.7	0.7	17.4	17.4	0.0
Bravo Big Bend, C67	WTX_2	50	0.5	0.4	-0.1	32.8	33.9	1.2	7.2	7.4	0.2

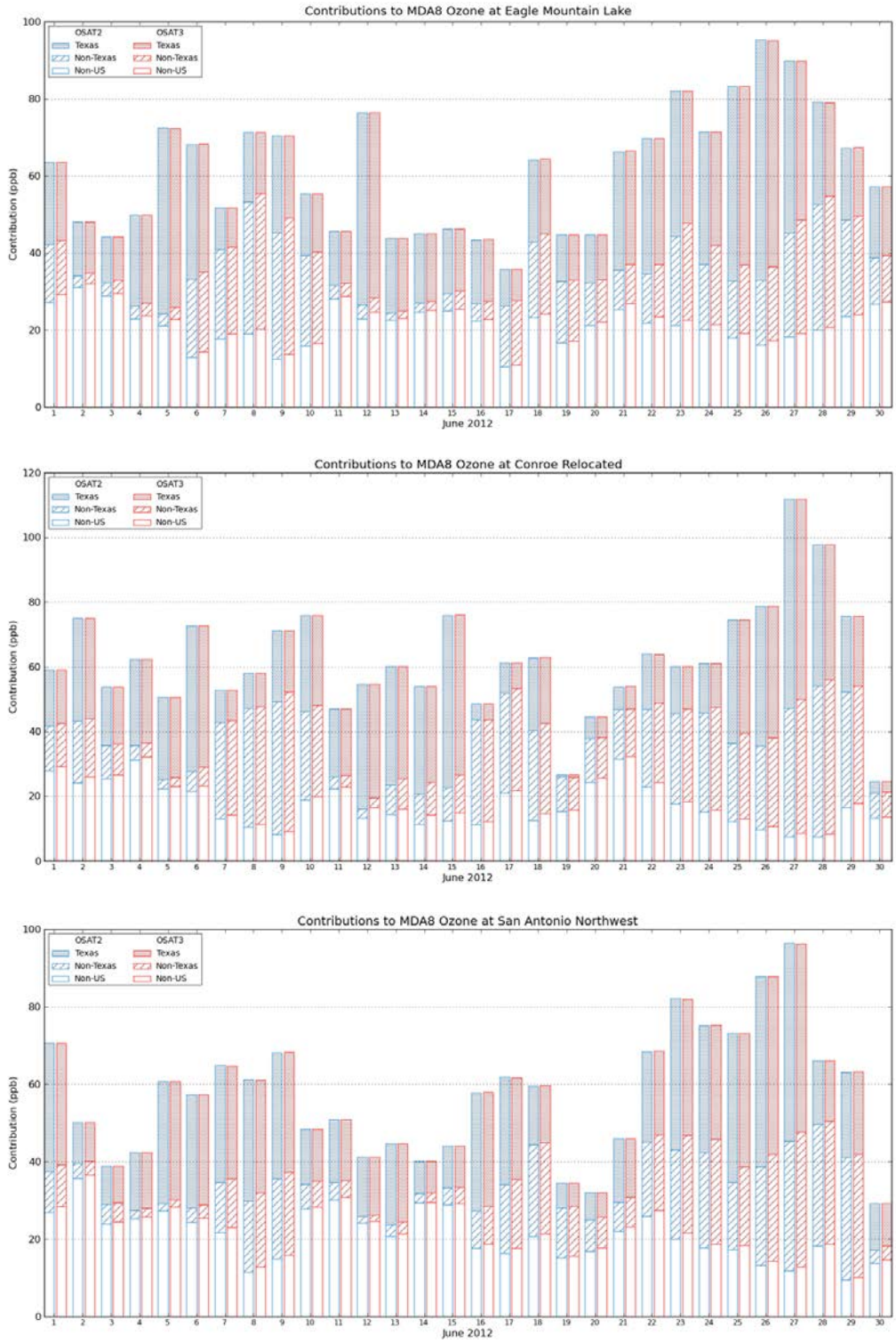

Figure 3-4. Contributions to daily MDA8 O_3 in June, 2012 from sources outside the US, outside Texas and within Texas at three monitors downwind of urban areas: Eagle Mountain Lake (CAMS 75; top), Conroe (CAMS 78; middle) and San Antonio Northwest (CAMS 23; bottom).

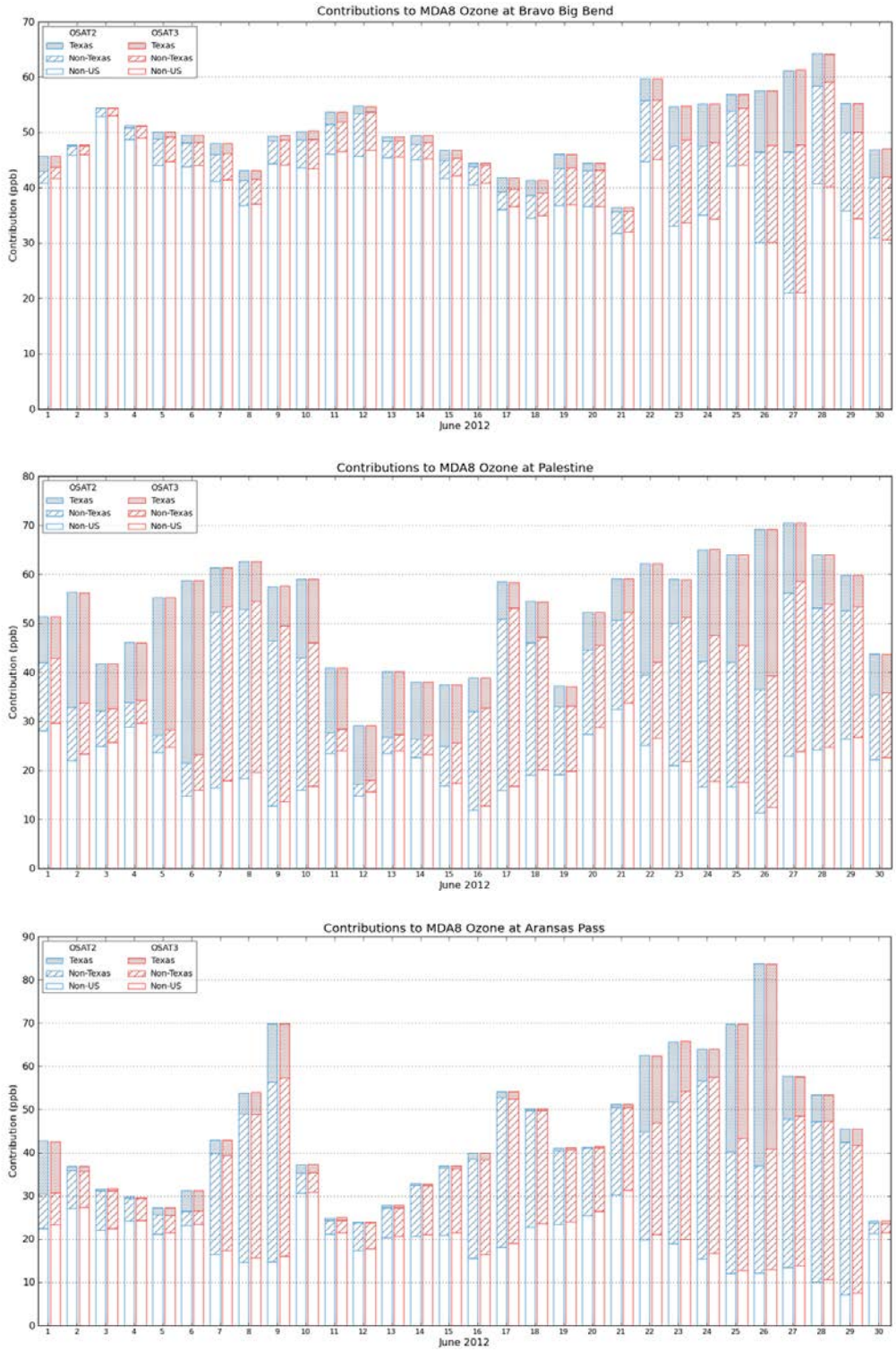

Figure 3-5. Contributions to daily MDA8 O_3 in June, 2012 from sources outside the US, outside Texas and within Texas at three monitors in rural areas: Big Bend (CAMS 67; top), Palestine (CAMS 647; middle) and Aransas Pass (CAMS 659; bottom).

The modifications in OSAT3 improve the accuracy of the O_3 source apportionment in two ways:

- By keeping track of the source(s) of O_3 removed by reaction with NO to form NO_2 and subsequently returned as O_3 when the NO_2 is destroyed by photolysis.
- By keeping track of so-called "NOx recycling," when NOx is converted to a different form of oxidized nitrogen, such as NHO_3, and later converted back to NOx.

Differences in O_3 source apportionment due to both updates are apparent downwind of Houston.

Figure 3-6 shows the OSAT3 tracers for O_3, NO_2 (i.e., RGN) and odd-oxygen in NO_2 (i.e., OON plus OOV) from Houston area emissions at 06:00 CST on June 14, 2012. The plume of O_3 from Houston emissions passed over the DFW metro area causing Houston O_3 to react with DFW NO emissions and form NO_2. The odd-oxygen in this NO_2 is attributed to Houston the area causing a local maximum over DFW in the tracer for odd-oxygen in NO_2 (i.e., OON plus OOV) from Houston O_3. From 06:00 and 07:00 CST, sunlight increased and NO_2 was destroyed by photolysis causing the tracer for odd-oxygen in NO_2 from Houston O_3 to decrease (Figure 3-7) and regenerate O_3 that was attributed to the Houston area, as seen from the difference in O_3 attributed to Houston between OSAT3 and OSAT2 (Figure 3-7). The O_3 attributed to Houston differs between OSAT3 and OSAT2 because OSAT3 attributes O_3 formed from destruction of NO_2 to the sources of odd-oxygen in the NO_2 destroyed whereas OSAT2 lacks this capability.

Figure 3-8 shows the OSAT3 tracers for O_3 (i.e., O3N plus O3V) and PAN (i.e., TPN) attributed to Houston area emissions at 11:00 and 13:00 CST on June 16, 2012. A plume of O_3 and PAN attributed to Houston area emissions extends north across Texas and Oklahoma. From, 11:00 and 13:00 CST, the PAN from Houston area emissions decreased over Oklahoma, due to thermal decomposition of PAN, and the NO_2 released was available to participate in O_3 formation. Consequently, the O_3 attributed to Houston area emissions by OSAT3 increased over Oklahoma, as seen from the O_3 difference between OSAT3 and OSAT2, because OSAT3 accounts for NOx recycled from PAN and subsequent O_3 production from the NOx.

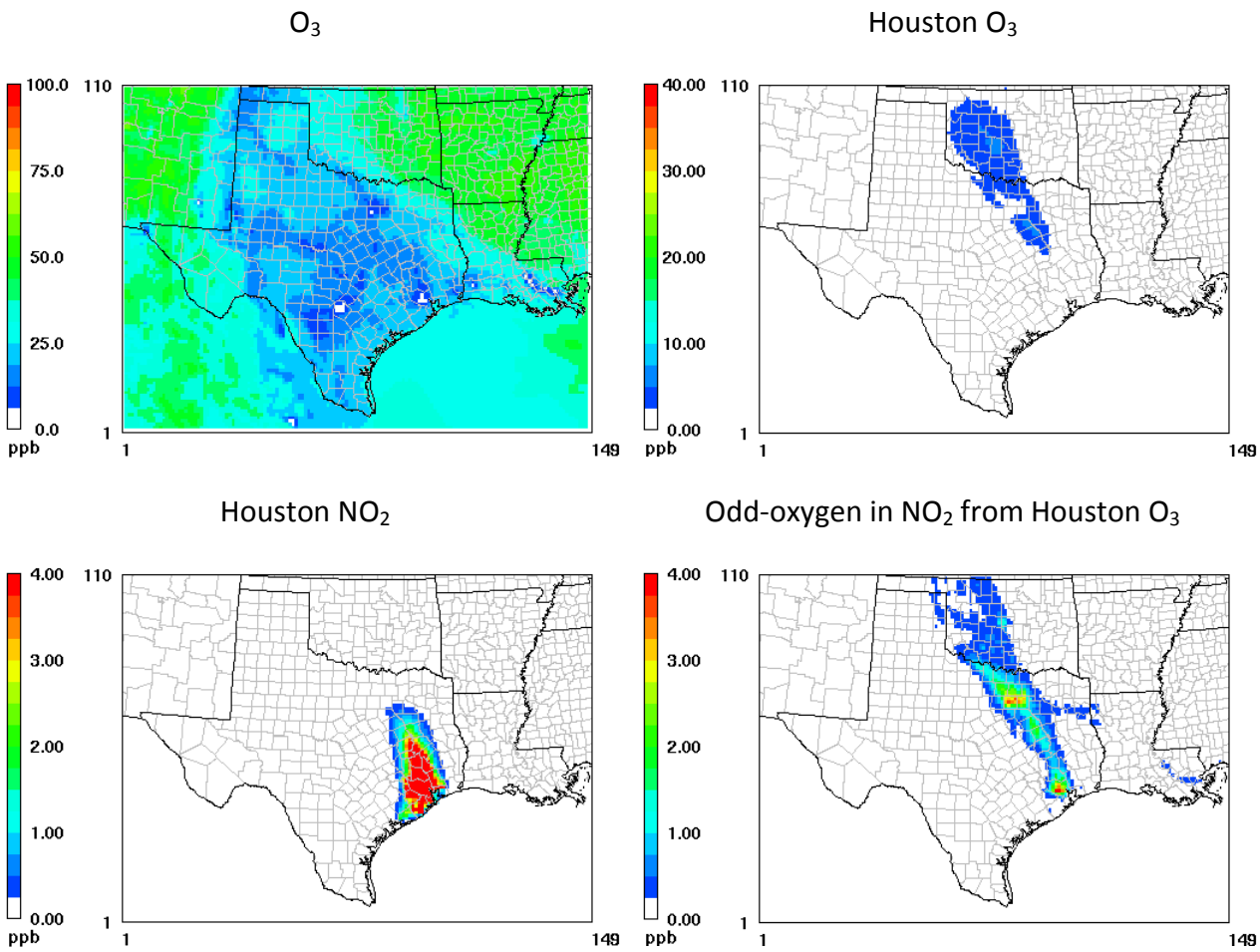

Figure 3-6. Hourly O_3 and OSAT3 tracers for Houston area emissions at 06:00 CST on June 14, 2012. Where the plume of O_3 from Houston emissions passes over the DFW metro area, a local minimum occurs where Houston O_3 has reacted with DFW NO emissions causing a local maximum in the tracer for odd-oxygen in NO_2 from Houston O_3. The tracer for Houston NO_2 has a different footprint because it traces the origin of nitrogen rather than the odd-oxygen in NO_2.

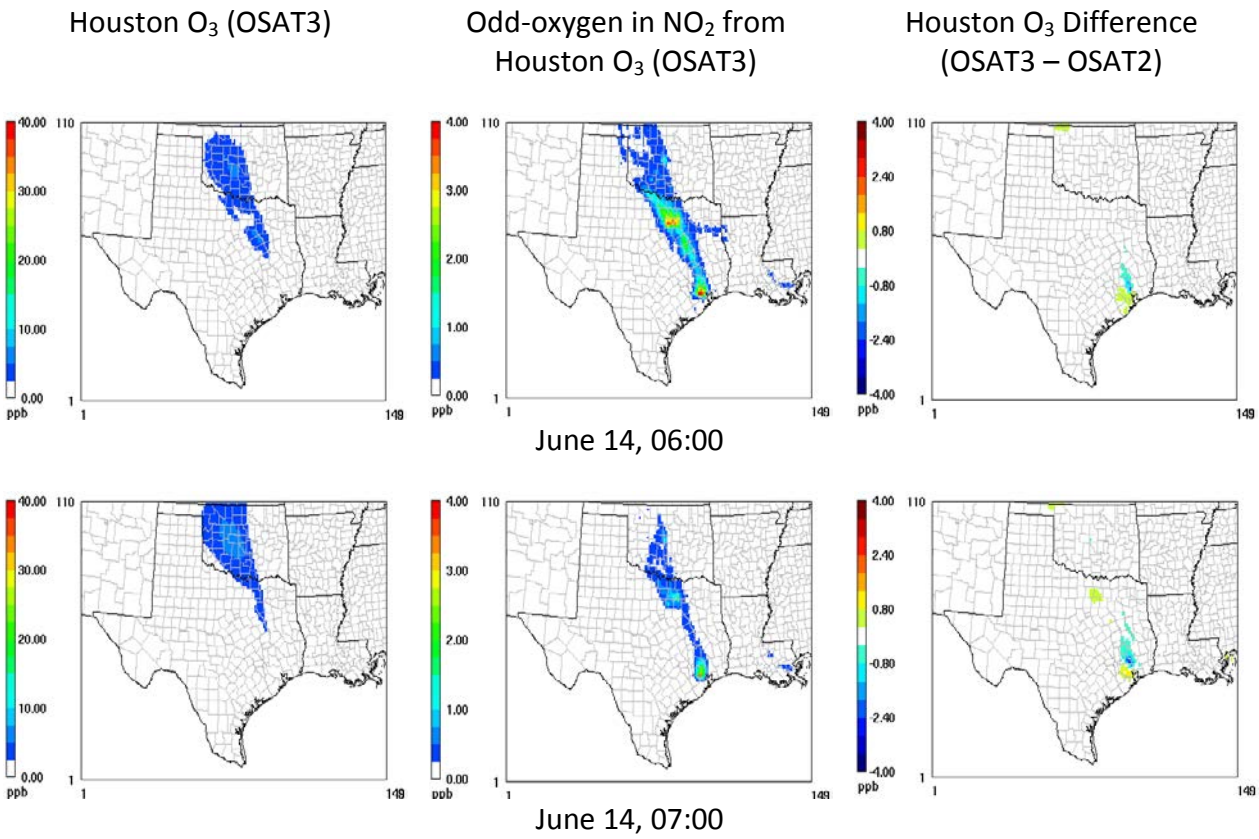

Figure 3-7. Hourly O_3 and OSAT3 tracers for Houston area emissions at 06:00 and 07:00 CST on June 14, 2012. Over the DFW metro area, decreases in the tracer for odd-oxygen in NO_2 from Houston O_3 coincide with increases in Houston O_3, as seen from the difference between OSAT3 and OSAT2, because OSAT3 attributes O_3 formed from destruction of NO_2 to the sources of odd-oxygen in the NO_2 destroyed.

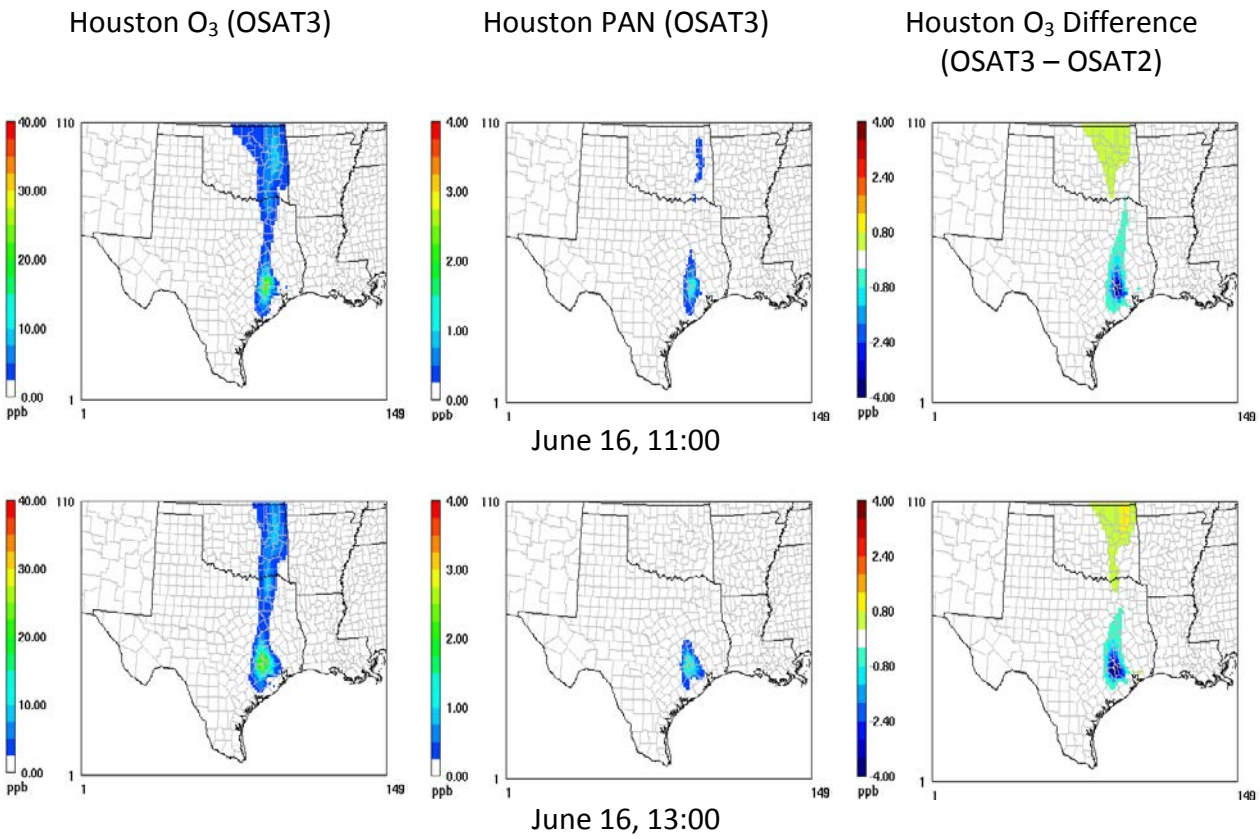

Figure 3-8. Hourly O_3 and PAN attributed to Houston area emissions at 11:00 and 13:00 CST on June 16, 2012. In Oklahoma, decreased PAN corresponds to increased O_3 with OSAT3, as seen from the O_3 difference between OSAT3 and OSAT2, because OSAT3 accounts for NOx recycled from PAN and subsequent O_3 production from the NOx.

4.0 CONCLUSION AND RECOMMENDATIONS

In this project the OSAT methods (OSAT, APCA and PSAT) were successfully updated to include source apportionment of NO_2. The sources of both the nitrogen atom and the odd oxygen in NO_2 are attributed, and these source profiles will almost always differ. The modifications improve the accuracy of the O_3 source apportionment in two ways:

- By keeping track of the source(s) of O_3 removed by reaction with NO to form NO_2 and subsequently returned as O_3 when the NO_2 is destroyed by photolysis.
- By keeping track of so-called "NOx recycling," when NOx is converted to a different form of oxidized nitrogen, such as NHO_3, and later converted back to NOx.

The effect of these updates on ozone source attribution is that the contribution of local emissions generally is reduced and the contribution of transported O_3 generally is increased.

4.1 Recommendations

Source apportionment is difficult to obtain for secondary pollutants that have non-linear relationships with their emitted precursor(s). The OSAT methods have proven to be useful because they are computationally efficient, flexible, and give answers that make sense when compared to other methods (e.g., setting emissions to zero one sector at a time). Recently, a new method was developed, called the path-integral method (PIM; Dunker, Koo and Yarwood, 2015), that can produce information similar to the OSAT methods using mathematically rigorous equations. It would be useful to compare results from the PIM and OSAT for model applications in Texas.

5.0 REFERENCES

Bey, I., D. J. Jacob, R. M. Yantosca, J. A. Logan, B. Field, A. M. Fiore, Q. Li, H. Liu, L. J. Mickley, and M. Schultz. 2001. Global modeling of tropospheric chemistry with assimilated meteorology: Model description and evaluation, *J. Geophys. Res*., 106, 23,073-23,096.

Dunker, A.M., B. Koo, and G. Yarwood. 2015. Source apportionment of the anthropogenic increment to ozone, formaldehyde and nitrogen dioxide by the path-integral method in a 3-D model. Environmental Science & Technology, 49(11):6751-9. doi: 10.1021/acs.est.5b00467.

ENVIRON, 2015. The Comprehensive Air quality Model with extensions (CAMx), version 6.20. (Available from http://www.camx.com).

Guenther, A. B., X. Jiang, C. L. Heald, T. Sakulyanontvittaya, T. Duhl, L. K. Emmons, and X. Wang. "The Model of Emissions of Gases and Aerosols from Nature version 2.1 (MEGAN2. 1): an extended and updated framework for modeling biogenic emissions." Geoscientific Model Development 5, no. 6 (2012): 1471-1492. Doi: 10.5194/gmd-5-1471-2012

Sillman, S. 1995. The Use of NOy, H_2O_2, and HNO_3 as Indicators for Ozone - NOx-Hydrocarbon Sensitivity in Urban Locations. J. Geophys. Res., 100, 14,175-14,188.

Skamarock, W. C., J. B. Klemp, J. Dudhia, D. O. Gill, D. M. Barker, W. Wang, and J. G. Powers, 2005. "A description of the Advanced Research WRF Version 2". NCAR Tech Notes-468+STR. (Available from http://www.mmm.ucar.edu/wrf/users/docs/arw_v2.pdf).

Yarwood, G., R.E. Morris, M.A. Yocke, H. Hogo and T. Chico. 1996. Development of a Methodology for Source Apportionment of Ozone Concentration Estimates from a Photochemical Grid Model. Presented at the 89th AWMA Annual Meeting, Nashville TN, June 23-28.

Yarwood, G., R.E. Morris, G.M. Wilson. 2004. Particulate Matter Source Apportionment Technology (PSAT) in the CAMx Photochemical Grid Model. Proceedings of the 27th NATO/ CCMS International Technical Meeting on Air Pollution Modeling and Application. Springer Verlag (Available from http://www.camx.com/publ/pdfs/yarwood_itm_paper.pdf).